Small Wearable Meta Materials Antennas for Medical Systems

Albert Sabban

Department of Electrical Engineering
Ort Braude College, Karmiel, 2161002, Israel
sabban@netvision.net.il

Abstract ─ Communication industry is in rapid growth in the last years. Efficient small antennas are crucial in the development of medical systems. Low efficiency is the major disadvantage of small antennas. Meta material technology is used to improve the efficiency of small antennas. Design tradeoffs, computed and measured results of wearable meta-materials antennas with high efficiency are presented in this paper. All antennas were analyzed by using 3D full-wave software, ADS. The antennas electrical parameters on the human body are presented. The gain and directivity of the patch antenna with split-ring resonators, SRR, is higher by 2.5 dB than the patch antenna without SRR. The resonant frequency of the antennas with SRR is lower by 5% to 10% than the antennas without SRR. The resonant frequency of the antenna with SRR on human body is shifted by 3%.

Index Terms ─ Metamaterial antennas, printed antennas.

I. INTRODUCTION

Printed antennas are widely used in communication systems. Features of microstrip antennas such as low profile, flexible, light weight, compact and low production cost are crucial for wireless systems. Compact printed antennas are presented in journals and books, as referred in [1]-[4]. However, small printed antennas suffer from low efficiency. Meta material technology is used to design small printed antennas with high efficiency. Printed wearable antennas were presented in [5]. Artificial media with negative dielectric permittivity were presented in [6]. Periodic SRR and metallic posts structures may be used to design materials with dielectric constant and permeability less than 1 as presented in [6]-[14]. In this paper, meta-material technology is used to develop small antennas with high efficiency. Electrical properties of human tissues have been investigated in several papers such as [15-16]. Wearable antennas have been presented in papers in the last years as referred in [17-23]. The computed and measured bandwidth of the antenna with SRR and metallic strips is around 50% for VSWR of 2.3:1.

II. ANTENNAS WITH SRR

A microstrip printed antenna with SRR is shown in Fig. 1. The microstrip loaded dipole antenna with SRR in Fig. 1 provides horizontal polarization. The slot antenna provides vertical polarization. The resonant frequency of the antenna with SRR is 400 MHz. The resonant frequency of the antenna without SRR is 10% higher. The antennas shown in Fig. 1 consist of two layers. The dipole feed network is printed on the first layer. The radiating dipole with SRR is printed on the second layer. The thickness of each layer is 0.8 mm. The dipole and the slot antenna create dual polarized antenna. The computed S11 and antenna gain are presented in Fig. 2. The length of the antenna shown in Fig. 1 is 19.8 cm.

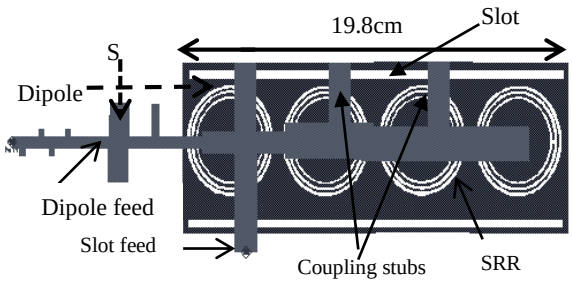

Fig. 1. Printed antenna with split ring resonators.

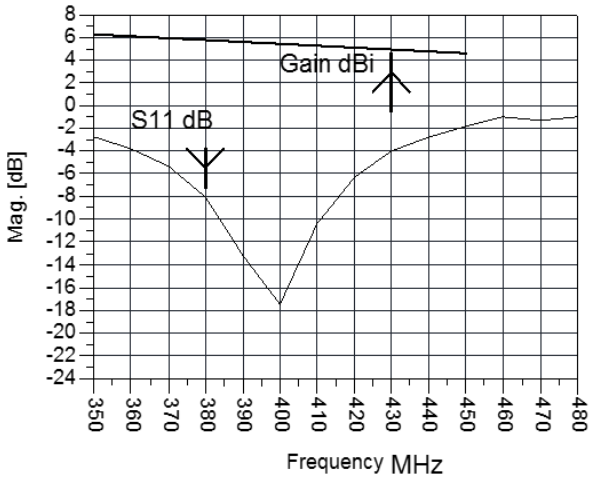

Fig. 2. Antenna with SRR, computed S11.

Submitted On: November 6, 2014
Accepted On: February 20, 2016

The length of the antenna without SRR is 21 cm as presented in [5]. The ring width is 1.4 mm the spacing between the rings is 1.4 mm. The antennas was designed by using ADS software. Directivity and gain of the antenna with SRR is around 5.5 dBi. Location and dimensions of the matching stubs was tuned to get the best VSWR results for the antennas presented in Fig. 1 and Fig. 3. The length of the stub S is 10 mm. The antenna axial ratio may be varied from 0 dB to 30 dB by optimizing the locations and the number of the coupling stubs. The number of coupling stubs in Fig 1 is three. Moreover, the antenna axial ratio value may be tuned by varying the position of the slot feed line. The measured bandwidth of the antenna without SRR is around 10% for VSWR better than 2:1. The antenna beam width is 100º. The antenna gain is around 2d Bi to 3 dBi. There is a good agreement between measured and computed results. The antenna presented in Fig. 1 has been modified as shown in Fig. 3. The location and the dimension of the coupling stubs have been modified to get wider bandwidth as shown in Fig. 4. The location and the dimension of the coupling stubs in Fig. 1 were optimized, as shown in Fig. 5, to get two resonant frequencies.

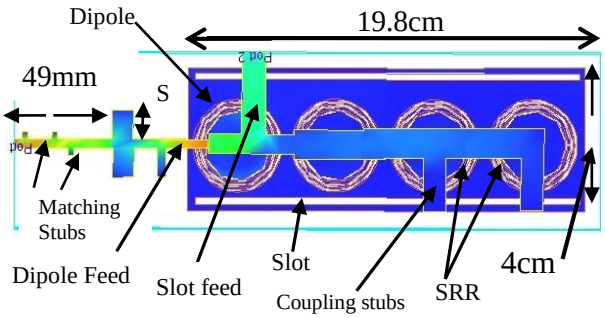

Fig. 3. Current distribution of the modified antenna.

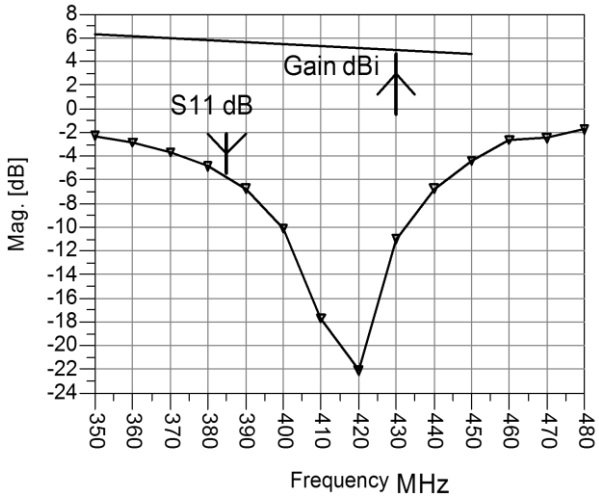

Fig. 4. Measured S11of the antenna without SRR.

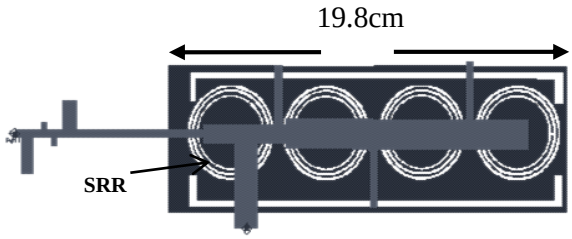

Fig. 5. Antenna with SRR with two resonant frequencies.

The first resonant frequency is 370 MHz, as shown in Fig. 6. Metallic strips have been added to the antenna with SRR as presented in Fig. 7. The antenna gain and computed S11 of the antenna with metallic strips is presented in Fig. 8. The antenna bandwidth is around 40% for VSWR better than 2.5:1. The 3D computed radiation pattern is shown in Fig. 9. Directivity and gain of the antenna with SRR is around 5.5dBi as shown in Fig. 10. The length of the antennas with SRR is smaller by 5% than the antennas without SRR. Moreover, the resonant frequency of the antennas with SRR is lower by 5% to 10%. The feed network of the antenna in Fig. 7 was optimized to yield VSWR better than 2:1 in frequency range of 250 MHz to 420 MHz as shown in Fig. 11. Optimization of the number of the coupling stubs and the distance between the coupling stubs may be used to tune the antenna resonant frequency. The current distribution along the antenna with SRR and two coupling stubs is shown in Fig. 12. The SRR have an important role in the radiation characteristics of the antenna. The antenna with two coupling stubs has two resonant frequencies. The first resonant frequency is 370 MHz and the second resonant frequency is 420 MHz.

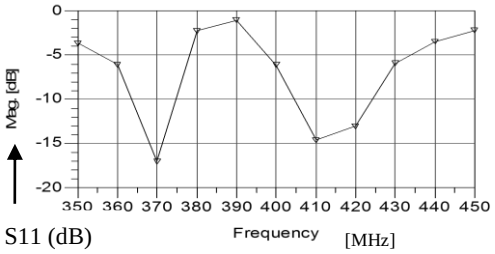

Fig. 6. S11 for antenna with two resonant frequencies.

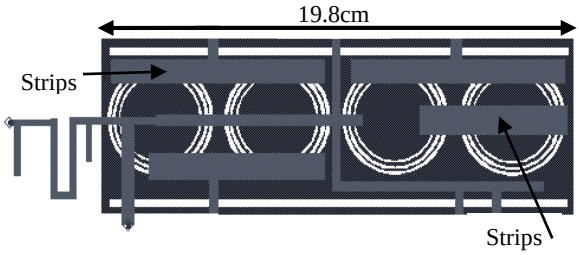

Fig. 7. Antenna with SRR and metallic strips.

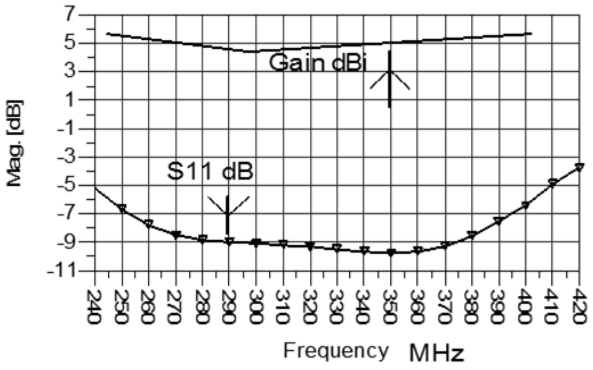

Fig. 8. S11 for antenna with SRR and metallic strips.

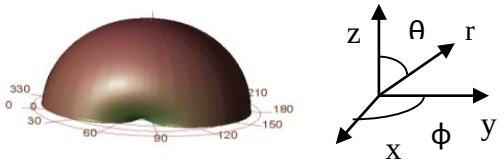

Fig. 9. 3D radiation pattern for antenna with SRR.

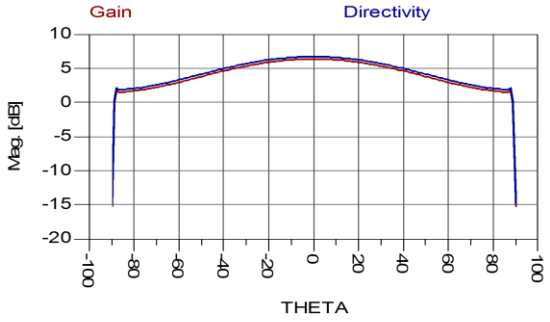

Fig. 10. Directivity of the antenna with SRR.

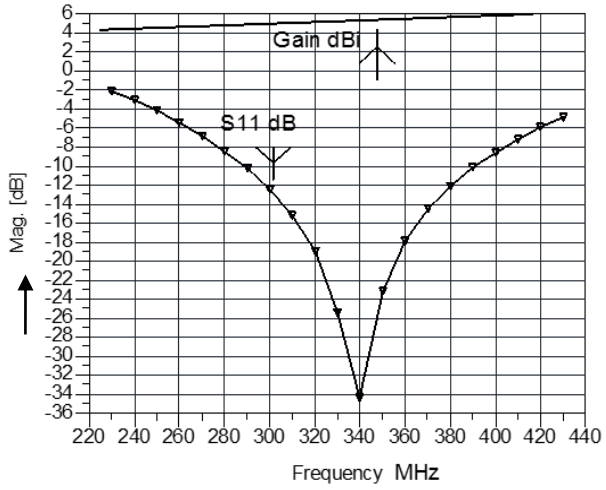

Fig. 11. S11 and gain for antenna with metallic strips.

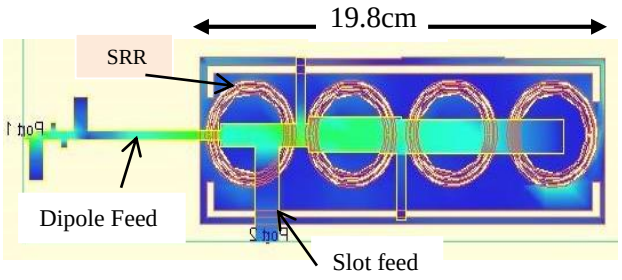

Fig. 12. Antenna with SRR with two coupling stubs.

The computed S11 parameter of the antenna with two coupling stubs is presented in Fig. 13. The 3D radiation pattern for antenna with two coupling stubs is shown in Fig. 14. The antenna with metallic strips was optimized to yield wider bandwidth as shown in Fig. 15. The S11 parameter of the modified antenna with metallic strips is presented in Fig. 16. The antenna bandwidth is around 50% for VSWR better than 2.3:1. Comparison between antennas with and without SRR is given in Table 1. The measured results agrees with the computed results.

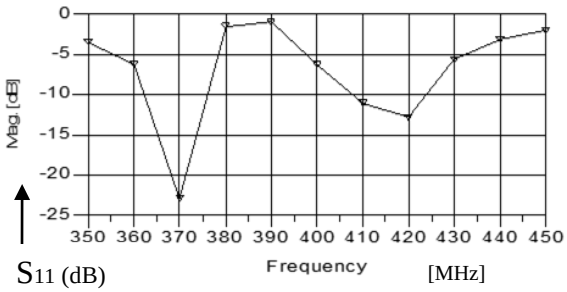

Fig. 13. S11 for antenna with two coupling stubs.

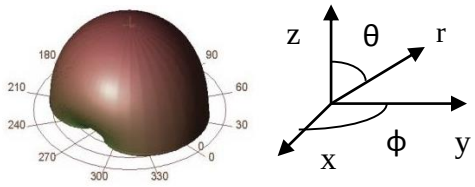

Fig. 14. 3D radiation pattern for antenna with SRR.

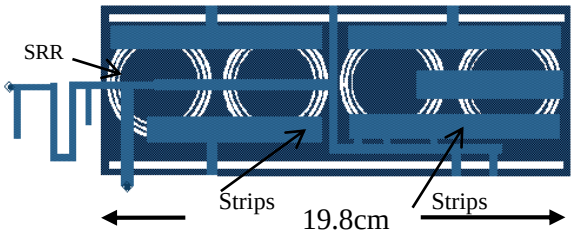

Fig. 15. Wideband antenna with SRR and metallic strips.

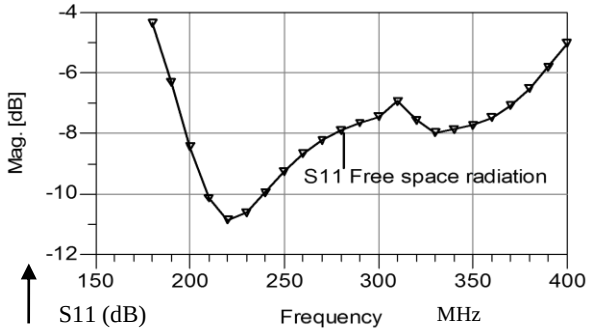

Fig. 16. S11 for antenna with SRR and metallic strips.

Table 1: Comparison between antennas with SRR

Antenna	Freq. (MHz)	VSWR %	Gain (dBi)	Length (cm)
With SRR	434	10	5.5	19.8
Without SRR	400	10	2.5	21
SRR and Strips	300	50	5.5	19.8

III. FOLDED DIPOLE META-MATERIAL ANTENNA WITH SRR

The length of the antenna shown in Fig. 1 may be reduced from 20 cm to 7 cm by folding the printed dipole as shown in Fig. 17. The antenna bandwidth is around 10% for VSWR better than 2:1. The antenna beam width is around 100º. The antenna gain is around 2 to 3 dBi. The size of the antenna with SRR shown in Fig. 1 may be reduced by folding the printed dipole as shown in Fig. 18. The dimensions of the folded dual polarized antenna with SRR presented in Fig. 18 are 11x11x0.16 cm. Figure 19 presents the antenna computed S11 parameters. The antenna bandwidth is 10% for VSWR better than 2:1. The computed radiation pattern of the folded antenna with SRR is shown in Fig. 20.

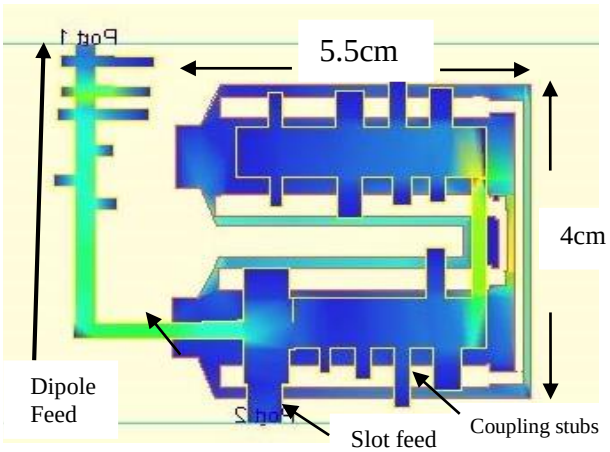

Fig. 17. Current distribution of the folded dipole.

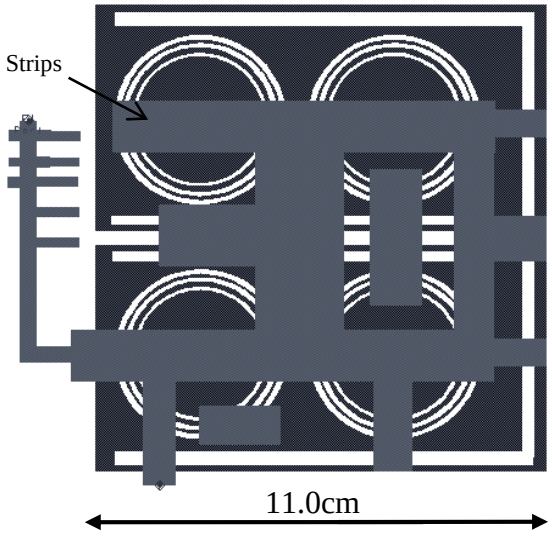

Fig. 18. Folded dual polarized antenna with SRR.

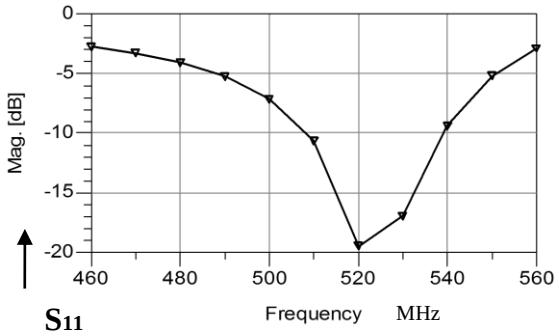

Fig. 19. Folded antenna with SRR, computed S11.

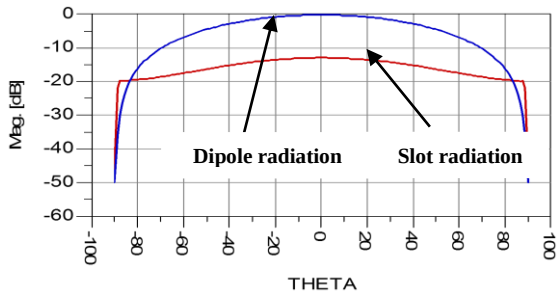

Fig. 20. Radiation pattern of the folded antenna with SRR.

IV. STACKED PATCH ANTENNA WITH SRR

At first a stacked patch antenna [1-3] has been designed. The second step was to design a patch antenna with SRR. The antenna consists of two layers. The first layer consists of FR4 substrate with dielectric constant

of 4. The second layer consists of RT-Duroid 5880 with dielectric constant of 2.2. The dimensions of the antenna shown in Fig. 21 are 33x20x3.2 mm. The antenna bandwidth is around 5% for VSWR better than 2.5:1. The antenna beam width is 72º.

The antenna gain is 7 dBi. The computed S11 parameters are presented in Fig. 22. Radiation pattern of the stacked patch is shown in Fig. 23. The antenna with SRR is shown in Fig. 24. This antenna has the same structure as the antenna shown in Fig. 21. The ring width is 0.2 mm the spacing between the rings is 0.25 mm. Twenty eight SRR are placed on the radiating element. There is a good agreement between measured and computed results. The measured S11 parameters of the antenna with SRR are presented in Fig. 25. The antenna bandwidth is around 12% for VSWR better than 2.5:1. By adding an air space of 4 mm between the antenna layers the VSWR was improved to 2:1. The antenna gain is around 9 to 10 dBi. The antenna computed radiation pattern is shown in Fig. 26. The antenna beam width is around 70º. The gain and directivity of the stacked patch antenna with SRR is higher by 2 dB to 3 dB than patch the antenna without SRR.

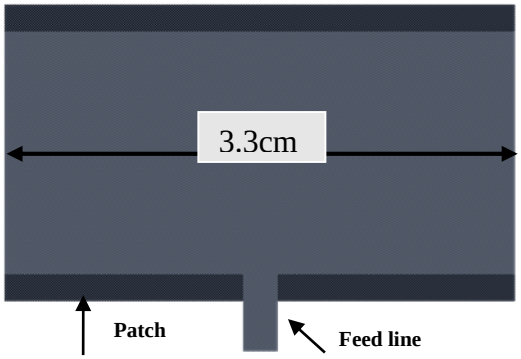

Fig. 21. A microstrip stacked patch antenna.

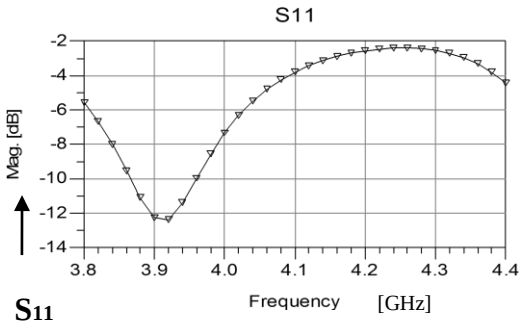

Fig. 22. Computed S11 of the microstrip stacked patch.

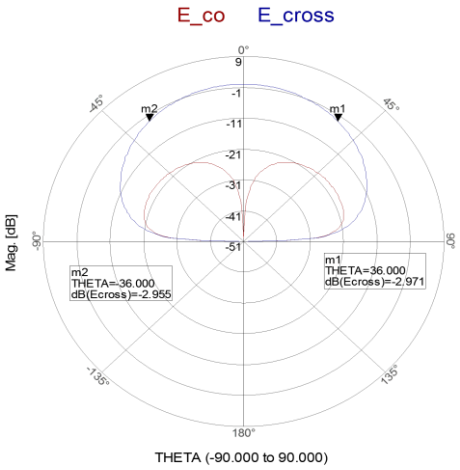

Fig. 23. Radiation pattern of the microstrip stacked patch.

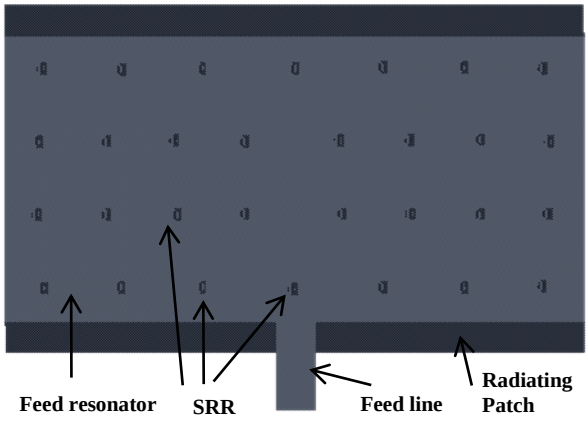

Fig. 24. Printed antenna with split ring resonators.

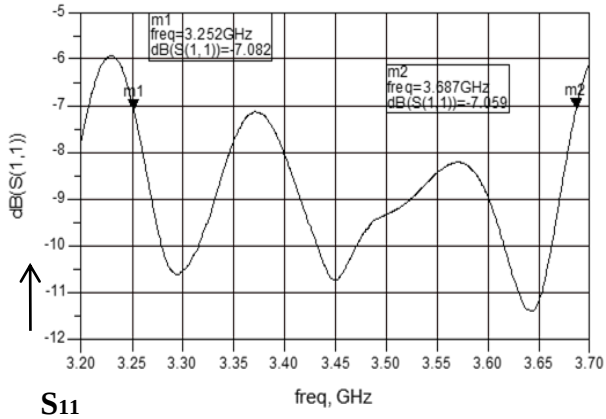

Fig. 25. Patch with split ring resonators, measured S11.

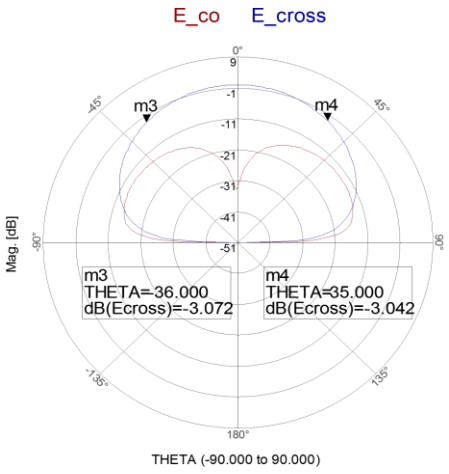

Fig. 26. Radiation pattern for patch with SRR.

V. PATCH ANTENNA LOADED WITH SRR

A patch antenna with split ring resonators has been designed. The antenna is printed on RT- DUROID 5880 dielectric substrate with dielectric constant of 2.2 and 1.6 mm thick. The dimensions of the microstrip patch antenna shown in Fig 27 are 33x16.6x3.2 mm. The antenna bandwidth is around 14% for S11 lower than -7.5 dB. The antenna bandwidth is 16% for VSWR better than 3:1. The antenna beam width is around 72º. The antenna gain is around 8 dBi. The computed S11 results are presented in Fig. 28. The gain and directivity of the antenna with SRR is higher by 3 dB than the patch antenna without SRR.

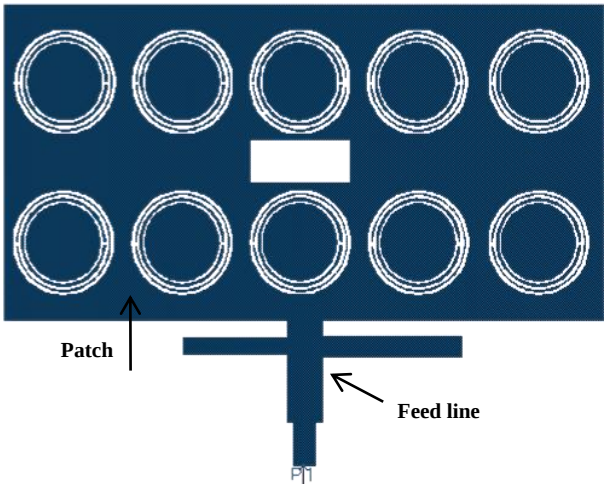

Fig. 27. Patch antenna with split ring resonators.

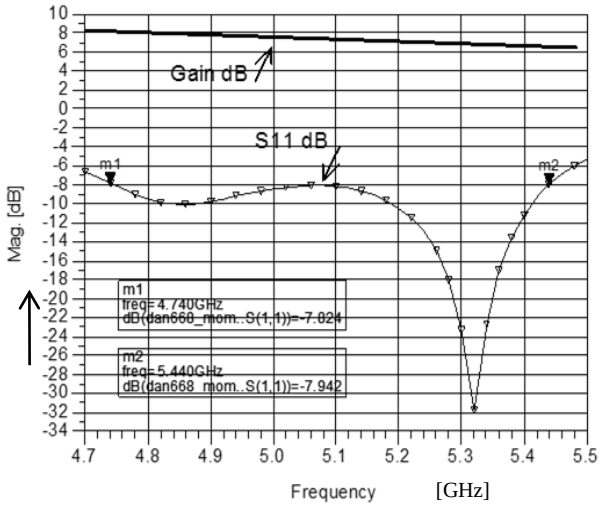

Fig. 28. Patch with SRR, computed S11.

VI. METAMATERIAL ANTENNAS IN VICINITY TO THE HUMAN BODY

The meta-materials antennas S11 variation in vicinity of the human body were computed by using the structure presented in Fig. 29 (a). Electrical properties of human body tissues are given in Table 2, see [15]. The antenna location on the human body is taken into account by computing S11 for different dielectric constant of the body tissues. The variation of the dielectric constant of the body from 43 at the stomach to 63 at the colon zone shifts the antenna resonant frequency by to 2%. The antenna was placed inside a belt with thickness between 1 to 4mm as shown in Fig. 29 (b). The belt dielectric constant was varied from 2 to 4. The antennas impedance was computed and measured for air spacing of 0 mm to 8 mm, between the patient shirt and the antennas. The dielectric constant of the patient shirt was varied from 2 to 4. Figure 30 presents S11 results of the antenna with SRR shown in Fig. 12 on the human body. The antenna resonant frequency is shifted by 3%. Figure 31 presents S11 results of the antenna with SRR and metallic strips, shown in Fig. 15. The antenna resonant frequency is shifted by 1%. Results presented in Fig. 31 indicate that the antenna has V.S.W.R better than 2.3:1 for 50% bandwidth. The radiation pattern of the antenna with SRR and metallic strips on human body is presented in Fig. 32. Figure 33 presents S11 results for different belt thickness, shirt thickness and air spacing between the antennas and human body for the antenna without SRR. One may conclude from results shown in Fig. 33 that, the antenna has S11 better than -9.5 dB for air spacing up to

8 mm between the antennas and the human body. Tunable wearable antenna may be used to control the antenna resonant frequency at different positions on the human body, see [24]. Figure 34 presents S11 results of the folded antenna with SRR, shown in Fig. 18, on the patient body. The antenna resonant frequency is shifted by 2%. The radiation pattern of the folded antenna with SRR on human body is presented in Fig. 35.

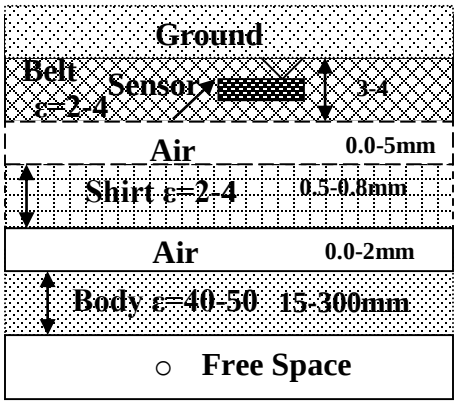

(a)

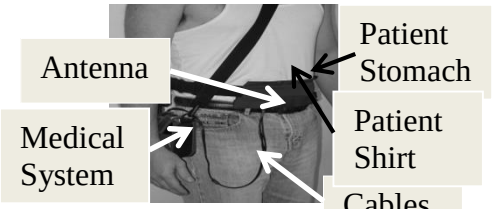

(b)

Fig. 29. (a) Antenna environment and (b) patient.

Table 2: Electrical properties of human body tissues

Tissue	Property	434 MHz	1200 MHz
Stomach	σ	0.67	0.97
	ε	42.9	39.06
Colon, muscle	σ	0.98	1.43
	ε	63.6	59.41
Fat	σ	0.045	0.056
	ε	5.02	4.58

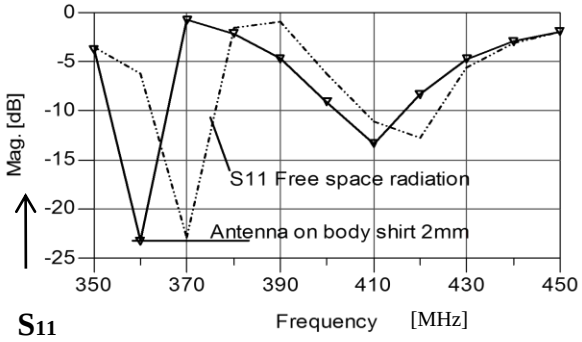

Fig. 30. S11 of the antenna with SRR on the human body.

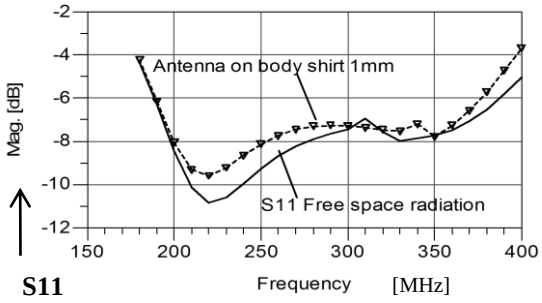

Fig. 31. Antenna with SRR S11 results on a patient.

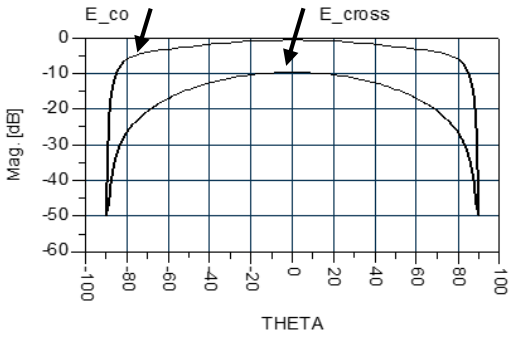

Fig. 32. Radiation pattern for antenna with SRR shown in Fig. 16 on the human body.

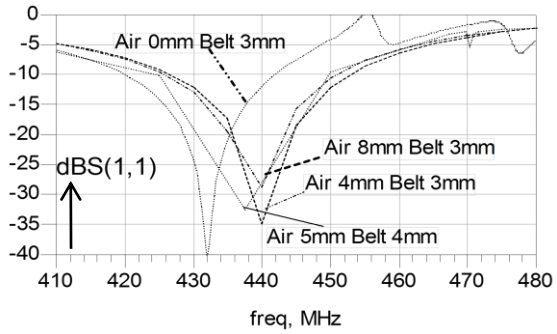

Fig. 33. S11 results for different locations relative to the human body for the antenna without SRR.

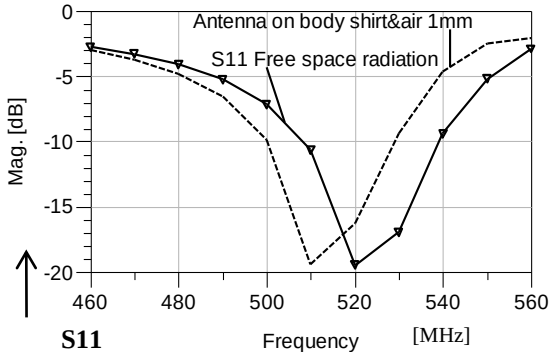

Fig. 34. Folded antenna with SRR, S11 on the body.

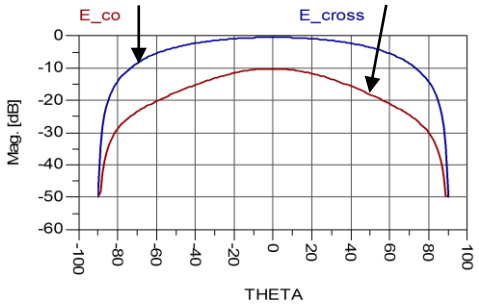

Fig. 35. Radiation pattern of the folded antenna with SRR on human body.

VII. METAMATERIAL WEARABLE ANTENNAS

The proposed meta-materials antennas may be placed on the patient body as shown in Fig. 36 (a). The patient in Fig. 36 (b) is wearing a wearable antenna. The antennas belt is attached to the patient front or back body. The cable from each antenna is connected to the medical system. The received signals are transferred via a SP8T switch to the receiver. The medical system selects the signal with the highest power. Usually the received signal during medical test with fat Persons is higher than the received signal during medical test with thin persons. The explanation is that the dielectric constant and conductivity of fat is much lower than the dielectric constant and conductivity of muscle and bone. The antennas electrical characteristics on human body have been measured by using a phantom that represents the human body electrical properties as presented in [5]. In several wearable systems the distance separating the transmitting and receiving antennas is in the near field zone. In the near-field area the antennas are magnetically coupled and only near field effects should be considered.

In the age of wireless products the proposed antennas are critical in developing efficient wearable systems. A photo of meta-material patch antenna with SRR is shown in Fig. 37.

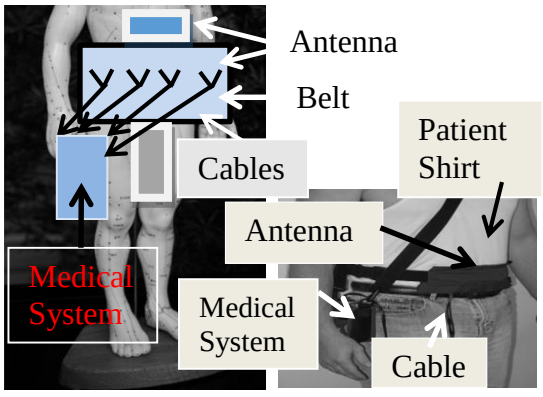

Fig. 36. (a) Medical system with wearable antennas, and (b) patient with printed wearable antenna.

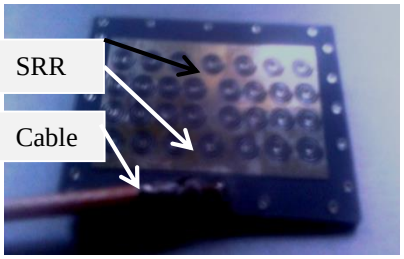

Fig. 37. Meta-material patch antenna with SRR.

VIII. ANALYSIS OF WEARABLE ANTENNAS

The major issue in the design of wearable antennas is the interaction between RF transmission and the human body. Electrical properties of human body tissues should be considered in the design of wearable antennas.

The dielectric constant and conductivity of human body tissues may be used to calculate the attenuation α of RF transmission through the human body. Figure 38 presents attenuation values of human tissues. Stomach tissue attenuation at 500 MHz is around 1.6 dB/cm. In Table 3 advantages of patch antennas with SRR is listed.

Results presented in Tables 1 and 3 show that antennas with SRR are more efficient, smaller and have a wider bandwidth than similar antennas without SRR. There is a good agreement between measured and computed results.

Table 3: Advantages of patch antennas with SRR

Patch\Value	Freq. (GHz)	Dimensions (mm)	VSWR 3:1	Gain dBi
Patch	3.9.5	36x20x3.2	2%	4.5
Patch with SRR	3.75	33x20x3.2	10%	7.5
Patch with SRR	5.1	33x16.6x3.2	14%	7.5
Stacked Patch	3.9	33x20x3.2	6%	7
Stacked Patch - SRR	3.5	33x20x3.2	12%	9.5

$$\gamma = \sqrt{j\omega\mu(\sigma + j\omega\varepsilon)} = \alpha + j\beta, \quad (1)$$

$$\alpha = Re(\gamma). \quad (2)$$

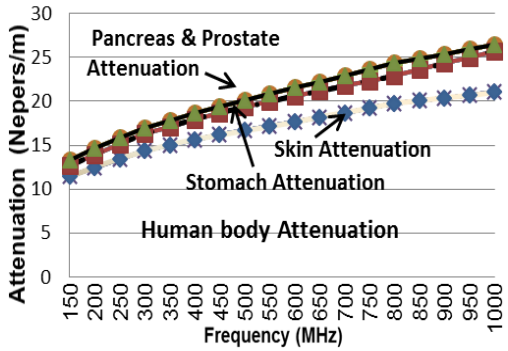

Fig. 38. Attenuation of human body tissues.

IX. CONCLUSION

Meta material technology is used to develop small antennas with high efficiency for medical systems. A new class of printed meta-materials antennas with high efficiency is presented. The bandwidth of the antenna with SRR and metallic strips is around 50% for VSWR better than 2.3:1. Optimization of the feed network, number of the coupling stubs and the length of the coupling stubs may be used to tune the antenna resonant frequency, radiation characteristics and the number of resonant frequencies. The length of the antennas with SRR is smaller by 5% than the antennas without SRR. Moreover, the resonant frequency of the antennas with SRR is lower by 5% to 10% than the antennas without SRR. The gain and directivity of the patch antenna with SRR is higher by 2 to 3 dB than the patch antenna without SRR. Measured results agrees with computed results.

REFERENCES

[1] J. R. James, P. S. Hall, and C. Wood, *Microstrip Antenna Theory and Design*, IEE, London, 1981.

[2] A. Sabban and K. C. Gupta, "Characterization of radiation loss from microstrip discontinuities using a multiport network modeling approach," *IEEE Trans. on M.T.T*, vol. 39, no. 4 , pp. 705-712, Apr. 1991.

[3] A. Sabban, "A new wideband stacked microstrip antenna," *IEEE Antenna and Propagation Symp*., Houston, Texas, U.S.A, June 1983.

[4] A. Sabban, *Microstrip Antenna Arrays*, *Microstrip Antennas*, Nasimuddin (Ed.), ISBN: 978-953-ISBN: 978-953-307-247-0, InTech, pp. 361-384, 2011.

[5] A. Sabban, "New wideband printed antennas for medical applications," *IEEE Journal, Trans. on Antennas and Propagation*, vol. 61, no. 1, pp. 84-91, Jan. 2013.

[6] J. B. Pendry, A. J. Holden, et al., "Extremely low frequency plasmons in metallic mesostructures," *Phys. Rev. Lett*., vol. 76, pp. 4773-4776, 1996.

[7] J. B. Pendry, A. J. Holden, et al., "Magnetism from conductors and enhanced nonlinear phenomena," *IEEE Trans. MTT*, vol. 47, pp. 2075-2084, 1999.

[8] R. Marque´s, F. Mesa, et al., "Comparative analysis of edge and broadside coupled split ring resonators for metamaterial design: Theory and experiment," *IEEE Trans. Antennas Propag*., vol. 51, pp. 2572-2581, 2003.

[9] R. Marque´s, J. D. Baena, et al., "Novel small resonant waveguides electromagnetic particles for metamaterial and filter design," *Phys. Rev. Lett*., vol. 89, Proc. ICEAA, pp. 439-442, Torino, Italy, 2003.

[10] R. Marque´s, J. Martel, et al., "Left-handed-media simulation and transmission of EM waves in sub wavelength split-ring-resonator loaded metallic waveguides," *Phys. Rev. Lett*., vol. 89, 2002.

[11] J. D. Baena, R. Marque´s, et al., "Experimental results on metamaterial simulation using SRR-loaded waveguides," I*EEE-AP/S Int. Symposium on, Antennas and Propagation Proc*., pp. 106-109, 2003.

[12] R. Marque´s, J. Martel, et al., "A new 2-D isotropic left-handed metamaterial design: Theory and experiment," *Microwave Opt. Tech. Lett*., vol. 35, pp. 405-408, 2002.

[13] R. A. Shelby, D. R. Smith, et al., "Microwave transmission through a two dimensional, left-handed meta-material," *Appl. Phys. Letters*, vol. 78, pp. 489-491, 2001.

[14] J. Zhu and G. V. Eleftheriades, "A compact transmission line metamaterial antenna with extended bandwidth," *IEEE Antennas and Wireless Propagation Wireless Propagation Letters*, vol. 8, 2009.

[15] L. C. Chirwa, et all., "Electromagnetic radiation from ingested sources in the human intestine between 150 MHz and 1.2 GHz," *IEEE Transaction on Biomedical Eng*., vol. 50, no. 4, pp. 484-492, Apr. 2003.

[16] D. Werber, A. Schwentner, and E. M. Biebl, "Investigation of RF transmission properties of human tissues," *Adv. Radio Sci*., 4, pp. 357-360, 2006.

[17] B. Gupta, S. Sankaralingam, et al., "Development of wearable and implantable antennas in the last decade," *Microwave Symposium (MMS), 2010*, Mediterranean, pp. 251-267, 2010.

[18] T. T. Z. Popovic, et al., "Investigation and design of a multi-band wearable antenna," *3rd European Conference on Antennas and Propagation, EuCAP 2009*, pp. 462-465, 2009.

[19] P. Salonen, Y. Rahmat-Samii, et al., "Wearable antennas in the vicinity of human body," *IEEE Antennas and Propagation Symp.*, vol. 1 pp. 467-470, July 2004.

[20] A. Sabban, "Wideband printed antennas for medical applications," *APMC Conference*, Singapore, Dec. 2009.

[21] A. Alomainy, A. Sani, et al., "Transient characteristics of wearable antennas and radio propagation channels for ultra-wideband body wireless communication," *IEEE Trans. on Antennas and Propagation*, vol. 57, no. 4, pp. 875-884, Apr. 2009.

[22] M. Klemm and G. Troester, "Textile UWB antenna for wireless body area networks," *IEEE Trans. on Antennas and Propagation*, vol. 54, no. 11, pp. 3192-3197, Nov. 2006.

[23] P. M. Izdebski, H. Rajagoplan, et al., "Conformal ingestible capsule antenna: A novel chandelier

meandered design," *IEEE Trans. on Antennas and Propagation*, vol. 57, no. 4, pp. 900-909, Apr. 2009.

[24] A. Sabban, "Wideband tunable printed antennas for medical applications," *IEEE Antenna and Propagation Symp*., Chicago, IL, USA, July 2012.

A. Sabban (M'87-SM'94) received the B.Sc. degree and M.Sc. degree Magna Cum Laude in Electrical Engineering from Tel Aviv University, Israel in 1976 and 1986 respectively. He received the Ph.D. degree in Electrical Engineering from Colorado University at Boulder, USA, in 1991. Sabban reasearch interests are microwave and antenna engineering. In 1976 he joined the armament development authority RAFAEL in Israel. In RAFAEL he worked as a Senior Researcher, Group Leader and Project Leader in the Electromagnetic Department till 2007. In 2007 he retired from RAFAEL. From 2008 to 2010 he worked as an RF Specialist and Project Leader in Hitech Companies. From 2010 to date he is a Senior Lecturer and Researcher in Ort Braude College in Israel in the Electrical Engineering Department. He published over 60 research papers and hold a patent in the antenna area. Sabban wrote two books on Low Visibilty Antennas and a book on Electrmagnetics and Microwave Theory for graduate students. He also wrote two chapters in books on Microstrip Antennas.